The effectiveness of three-dimensional reconstruction in the localization of multiple nodules in lung specimens: a prospective cohort study

Ying Ji[1], Tao Zhang[2], Lin Yang[3], Xin Wang[3], Linlin Qi[4], Fengwei Tan[1], Jean H. T. Daemen[5], Erik R. de Loos[5], Bin Qiu[1], Shugeng Gao[1]

[1]Department of Thoracic Surgery, National Cancer Center/National Clinical Research Center for Cancer/Cancer Hospital, Chinese Academy of Medical Sciences and Peking Union Medical College, Beijing, China; [2]Department of Radiotherapy, National Cancer Center/National Clinical Research Center for Cancer/Cancer Hospital, Chinese Academy of Medical Sciences and Peking Union Medical College, Beijing, China; [3]Department of Pathology, National Cancer Center/National Clinical Research Center for Cancer/Cancer Hospital, Chinese Academy of Medical Sciences and Peking Union Medical College, Beijing, China; [4]Department of Diagnostic Radiology, National Cancer Center/National Clinical Research Center for Cancer/Cancer Hospital, Chinese Academy of Medical Sciences and Peking Union Medical College, Beijing, China; [5]Department of Surgery, Division of General Thoracic Surgery, Zuyderland Medical Center, The Netherlands

Contributions: (I) Conception and design: B Qiu, Y Ji; (II) Administrative support: S Gao; (III) Provision of study materials or patients: B Qiu, S Gao; (IV) Collection and assembly of data: Y Ji; (V) Data analysis and interpretation: Y Ji, X Wang, L Qi, JHT Daemen, ER de Loos; (VI) Manuscript writing: All authors/Both authors; (VII) Final approval of manuscript: All authors/Both authors.

Correspondence to: Shugeng Gao, MD; Bin Qiu, MD. Department of Thoracic Surgery, National Cancer Center/National Clinical Research Center for Cancer/Cancer Hospital, Chinese Academy of Medical Sciences and Peking Union Medical College, Beijing 100021, China. Email: gaoshugeng@vip.sina.com; drqiubin@aliyun.com.

Background: The detection rate of multiple pulmonary nodules in computed tomography (CT) screening has increased significantly in recent years. In cases with multiple nodules within the same lung lobe or segment, it is often difficult for thoracic surgeons and pathologists to accurately locate all lesions in the surgically resected specimens. Therefore, the objective of our study was to use three-dimensional (3D) reconstruction in conjunction with 3D printing as an auxiliary method for localizing multiple small nodules in specimens after surgery and to evaluate its effectiveness.

Methods: A single-center prospective cohort study was conducted between September 2019 and September 2020 at the National Cancer Center (Beijing, China). In total, 43 surgical candidates with multiple nodules were recruited to undergo lobectomy or segmentectomy and 40 patients were ultimately enrolled in this study. With the assistance of 3D reconstruction/printing models, the obtained specimens were marked and then identified by a pathologist. The primary outcome was the success rate of nodule localization in the resected specimens, and the secondary outcome was the agreement rate between the pathological results of the samples and CT images.

Results: In the 40 patients enrolled, 126 nodules were detected by preoperative imaging, of which 124 nodules (positive rate: 98.4%) were successfully located in the resected specimens using 3D reconstruction/ printing. For the 124 nodules, the agreement rate of the pathological results of samples and CT images with the assistance of 3D reconstruction/printing models was 100.0%.

Conclusions: The results show that 3D reconstruction/printing models allow for the rapid and accurate localization of nodules in resected specimens. Also, the pathological results of lesions show good agreement with the results of preoperative CT imaging, which is of great significance for further study into the clinicopathological characteristics and radiomics of multiple pulmonary nodules.

Keywords: Multiple nodules; three-dimensional (3D); pathological sampling

Introduction

Since the mid-20th century, evidence supporting the substantial contribution of lung cancer screening to the detection and treatment of precursor lesions has been accumulating (1,2). With the improvement in awareness of cancer prevention and the clinical application of high-resolution computed tomography (CT), the number of patients diagnosed with multiple pulmonary nodules has gradually increased (3-5). In most cases, the lesions of these patients show as pure ground-glass nodules (pGGNs) or mixed ground-glass nodules (mGGNs) on CT images. For most patients with multiple nodules, surgery constitutes an effective radical treatment, and wedge resection, anatomical segmentectomy or lobectomy should be selected according to the particular case. Besides, surgical specimens can provide more detailed pathological and genetic characterization for follow-up treatment and monitoring of multiple primary lung cancers (6,7).

The reliability of sampling tissue specimens with multiple nodules depends on the precise location of each nodule. The ability of the pathologist to accurately determine the size and type of different nodules under the microscope can assist in clarifying the nature of multiple lesions, which is of guiding significance for tumor staging (multiple primary or intrapulmonary metastasis). Moreover, the level of agreement between the pathological report and preoperative CT imaging results can be helpful in assessing the accuracy of preoperative imaging diagnosis and informing further research on multiple pulmonary nodules.

However, in practice, it is challenging for pathologists to locate all nodules in specimens owing to a lack of understanding of preoperative CT images. Moreover, due to a lack of accurate description of the location of individual nodules, pathological reports for multiple nodules often fail to correspond with the findings of preoperative imaging. Therefore, it is urgent to find a method that will not only assist surgeons and pathologists to localize all nodules in resected specimens, but will also help researchers to obtain good agreement between pathological and imaging features in future studies (7).

Three-dimensional (3D) reconstruction and 3D printing models can provide cross-reference to guide surgeons and pathologists in locating multiple lesions in tissue specimens.

We conducted a prospective cohort study to explore the performance of using 3D reconstruction/printing to locate synchronous multiple pulmonary nodules in resected specimens. This method may provide a novel perspective on the application of 3D reconstruction/3D printing models in pathology.

We present the following article in accordance with the STROBE reporting checklist (available at http://dx.doi.org/10.21037/tlcr-21-202).

Methods

Study design

This study was conducted between September 2019 and September 2020 at the National Cancer Center (Beijing, China). The present study was designed to assess the value of using 3D reconstruction/printing in locating synchronous multiple pulmonary nodules in resected specimens. The study protocol is set out in Appendix 1. The study complies with the Declaration of Helsinki (as revised in 2013) and was approved by the Ethics Committee of the Cancer Hospital at the Chinese Academy of Medical Sciences (approval no. 20/130-2326).

Inclusion and exclusion criteria

Patients with synchronous multiple pulmonary nodules who were scheduled for anatomical segmentectomy or lobectomy were assessed by a trained researcher (Y Ji) to evaluate their eligibility for inclusion. The 2 main inclusion criteria were: largest diameter of the main lesion on the lung window ≤20 mm; and 2 or more lesions present in the same lobe or segment. The 2 primary exclusion criteria were: multiple lesions suspected to be metastatic tumors by preoperative evaluation; and conversion to wedge resection during the operation. The detailed inclusion and exclusion criteria are described in Appendix 1. Informed consent was taken from all the patients.

Primary outcome and secondary outcome

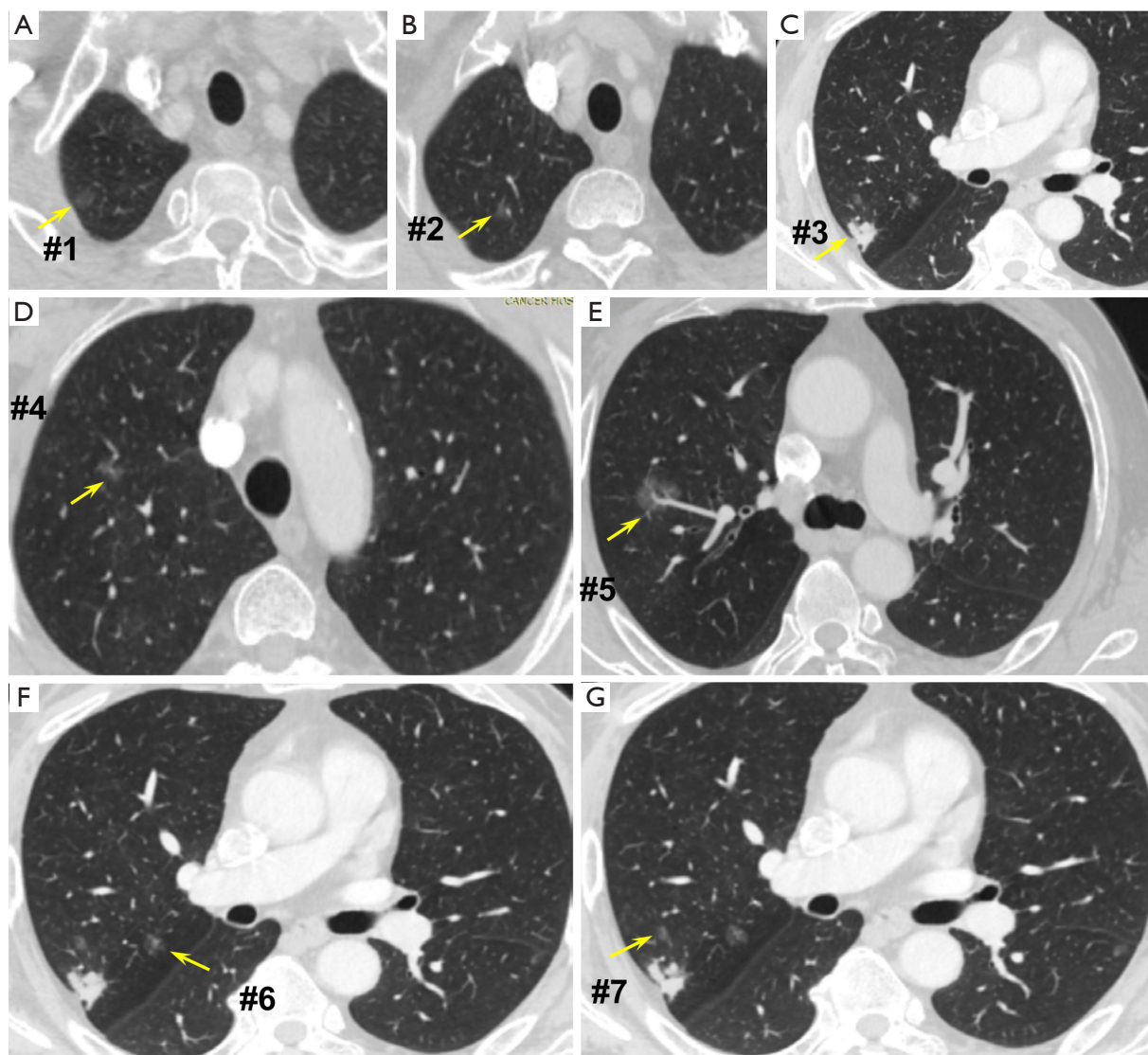The primary outcome was the success rate of nodule localization in the resected specimens, and the secondary

Figure 1 The CT scans of a patient with seven nodules (shown via yellow arrows) in right upper lobe who underwent lobectomy (A-G). Nodule #1 (A), #2 (B), #4 (D), #6 (F) and #7(G) show as pGGN; Nodule #5 (E) shows as PSN; Nodule #3 (C) shows as pure solid nodule.

outcome was the agreement rate between the pathological results of the samples and CT images.

The total number of nodules was defined as the number of nodules planned to be resected based on preoperative CT scan. The nodules were located with the auxiliary of personalized 3D reconstruction imaging after surgical resection of the specimens. After all nodules were identified on the surgical specimens, and the corresponding areas were marked with 4.0 silk suture. The procedural duration was calculated as the time between specimens were resected

and all nodules were labeled. Then, the labeled surgical specimens and the 3D printed models were sent to the Department of Pathology for sampling. The success rate of nodule localization was calculated as the ratio of the number of nodules actually localized to the total number of nodules based on preoperative imaging.

For example, *Figure 1* shows the CT images of a 66-year-old man with 7 nodules in the right upper lobe. The 3D reconstruction/printing image and surgical specimen of this case are shown in *Figure 2*. The pathologist diagnosed each
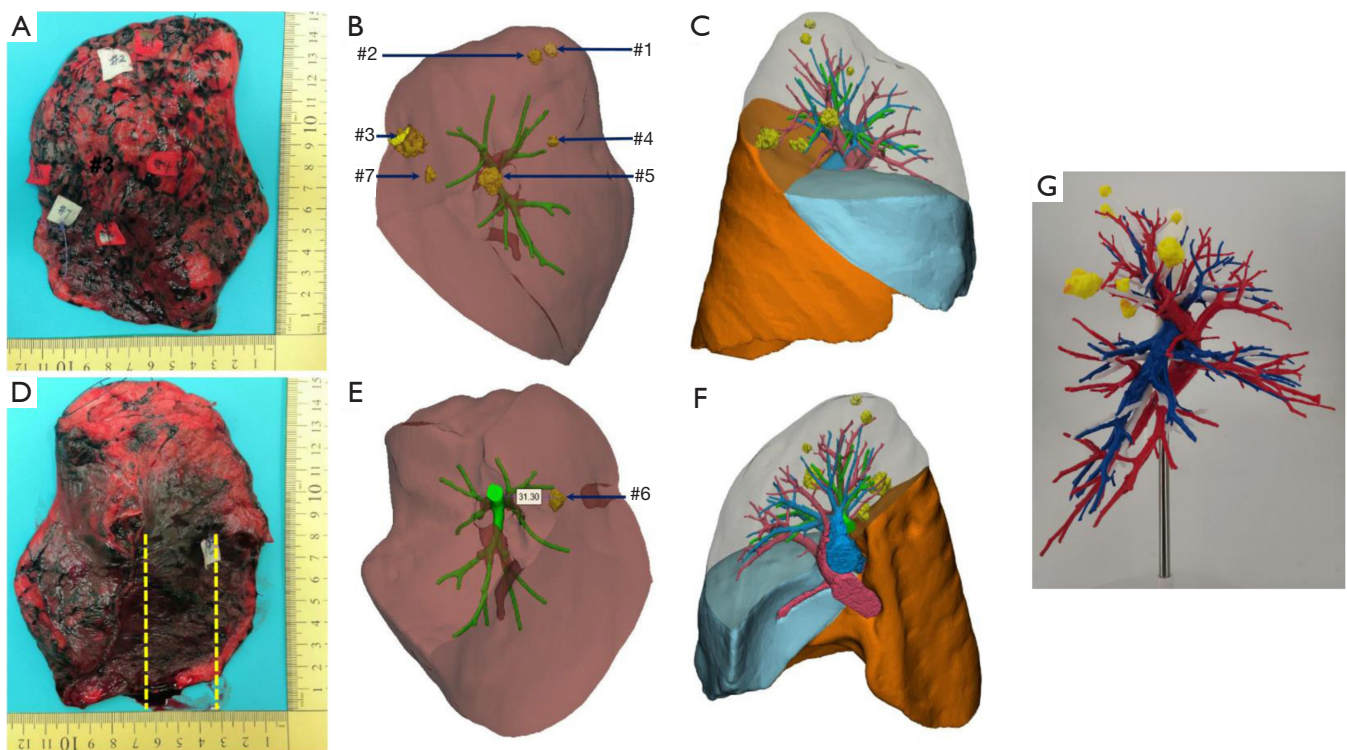
Figure 2 Matching personalized 3D reconstruction/3D printing model of the patient (which were shown in *Figure 1*) with the surgical specimen. (A,B,C) the frontal view of specimen and 3D reconstruction model; (D,E,F) the frontal view of specimen and 3D reconstruction model; (G) the personalized 3D printing model of the patient.

nodule according to the serial number (*Figure 3*).

Preoperative 3D image construction and 3D model printing

The preoperative CT data of each patient enrolled in our study were obtained from the imaging workstation in our institution. The assessment of lesion composition was performed by an experienced radiologist (L Qi). The digital imaging and communications in medicine (DICOM) data of thin-slice (0.625–1.25 mm) CT images were imported into Mimics Software for 3D reconstruction. In all 40 cases, the 3D models were printed after processing of the reconstruction images in the 'stereolithographic (stl)' format with 3-matic Software. All models were fabricated by ProJet MJP 3600 (3d systems, USA) with VisiJet Proplast. Stereo lithography Appearance (SLA) technology was used to complete entity printing.

Pathologic diagnosis

The pathologic diagnosis of lung cancer was based on the 2015 World Health Organization (WHO) classification for lung cancer, and the staging standard was based on the 8th editions of the International Union Against Cancer and American Joint Committee on Cancer (UICC/AJCC) TNM staging system for non-small cell lung cancer (8,9). All histologic preparations and analyses were performed by 2 senior pathologists majoring in lung cancer (L Yang and X Wang). In case of disagreement, mutual consensus was reached after discussion with other pathologists.

Statistical analysis

Normally distributed continuous variables are presented as mean ± standard deviation (SD), and continuous variables that were not normally distributed are presented as median and interquartile range (25th, 75th percentile). Normality
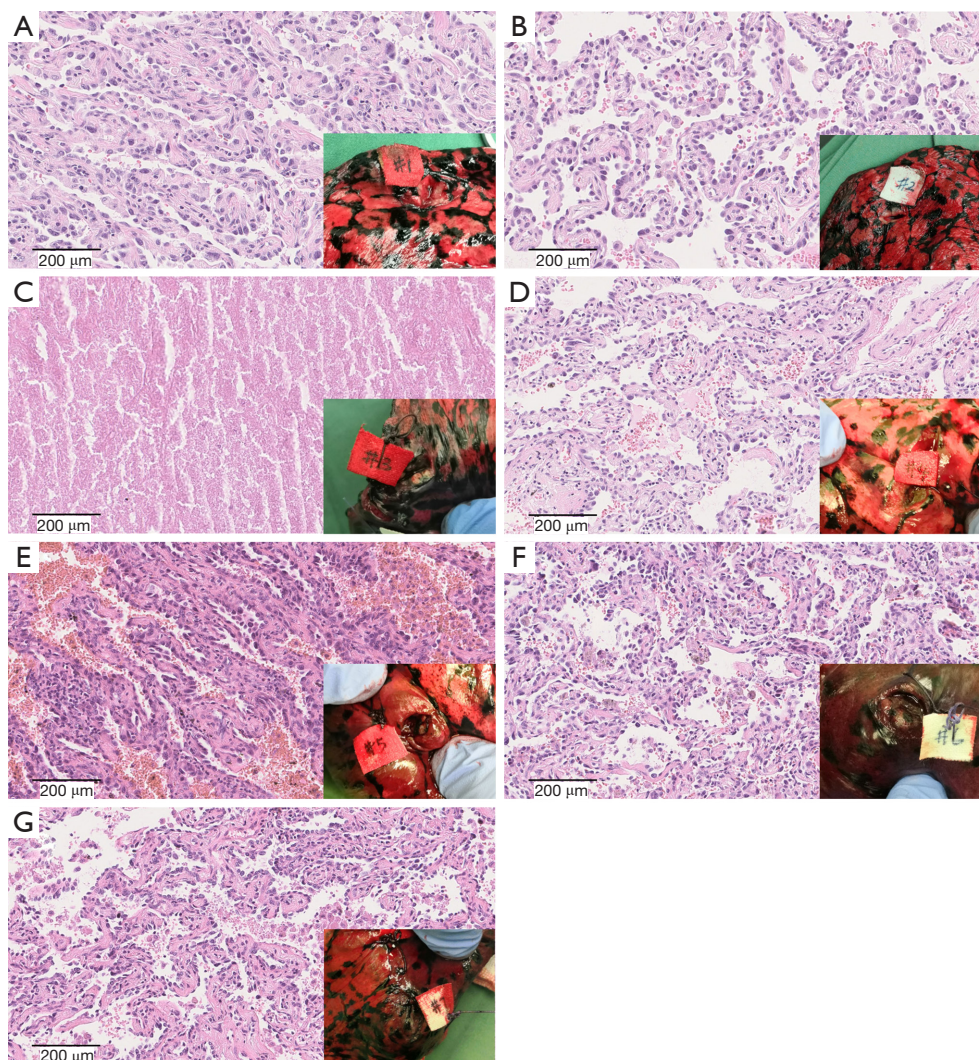
Figure 3 Pathological diagnosis of 7 nodules shown in *Figure 1* (HE staining). A-G corresponds to nodule #1-#7, respectively. (A) Adenocarcinoma *in situ*; (B) adenocarcinoma *in situ*; (C) necrotic nodule; (D) adenocarcinoma in situ; (E) invasive adenocarcinoma; (F) microinvasive adenocarcinoma; (G) microinvasive adenocarcinoma.

was assessed by the Shapiro-Wilk test and normal probability plot. Categorical variables are presented as frequency (percentage).

Results

In total, 43 patients with multiple pulmonary nodules treated in our hospital between September 1, 2019 and September 30, 2020 were eligible for inclusion in this study. Of them, 40 patients underwent lobectomy or anatomical segmentectomy were finally enrolled for analysis. A flowchart of participant enrollment is shown in *Figure 4*.

Patients characteristics

The 40 study participants included 9 male and 31 females, who had an average age of 53.5 (±8.5) years old. The 40 patients had a total of 126 nodules detected on CT, and the average lesion diameter was 9.8±4.2 mm. There were 98 (77.8%) pGGNs, 18 (14.3%) partial solid nodules (PSNs), and 10 (7.9%) pure solid nodules. The percentage of pGGNs is 70.4 (19/27) in male, while 79.8 (79/99) in female. For each patient, 1 or more lesions were not visible or could not be palpated on the surface of the surgically resected specimens. The median distance from the surface
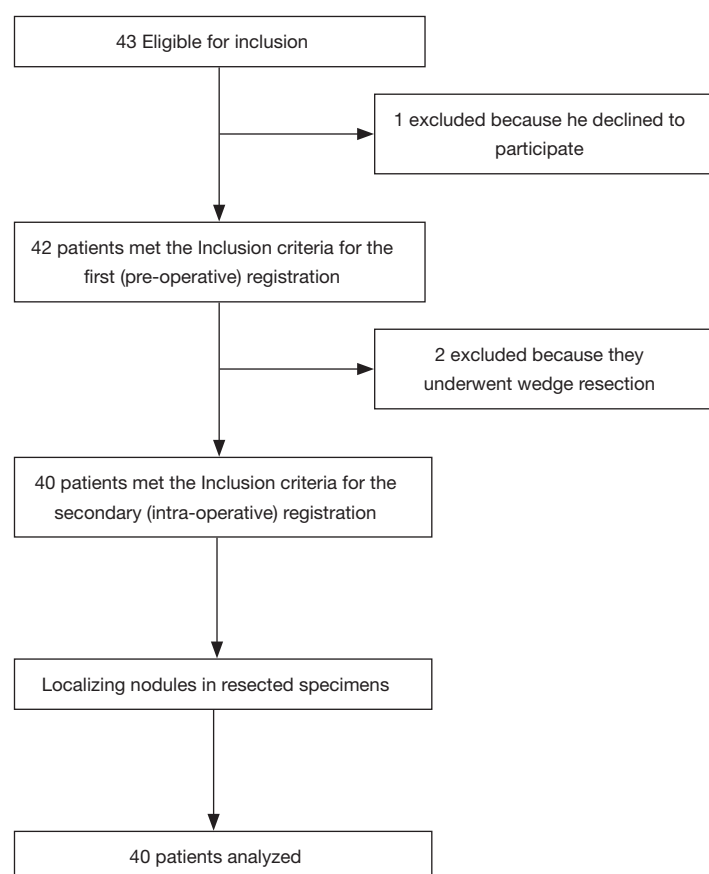
Figure 4 Flowchart of the study participants.

of the visceral pleura to the nodule was 8.2 mm (interquartile range, 25–75%, 4.8–11 mm) (*Table 1*). More details of each patient are shown in Table S1.

Characteristics of nodule localization

Of all 126 nodules of the 40 participants, 124 were successfully localized using the 3D reconstruction/printing models without sustaining damage. Thus, the success rate of nodule localization in the resected specimens was 98.4% (124/126). For the 124 successfully located nodules, the agreement rate of samples with CT images was 100% with the assistance of the 3D reconstruction/printing models. The mean procedural duration was 11 (±4.6) minutes (*Figure 5*).

Surgical and pathological results are summarized in *Table 2*. Two pGGNs were not found (one in the right upper lobe, measuring 4.2 mm in the largest dimension; and the other, in the right lower lobe, measuring 5.8 mm in the

largest dimension) (*Figure 6*).

Discussion

Multiple primary lung cancer is a common and complex type of lung cancer. Due to the substantial variability of tumor characteristics and the combination of different sites of lung cancer, the characteristics of these tumors are highly complex, which greatly increases the difficulty of prognostic research of multiple primary lung cancer (8). In the 8th edition of the TNM staging classification for lung cancer, the Staging and Prognostic Factors Committee (SPFC) of the AJCC divides multiple pulmonary sites of lung cancer into the following 4 patterns: second primary lung cancers; multiple lung cancer nodules with prominent ground glass or lepidic (GG/L) features; lung cancer that is radiologically similar to pneumonia (i.e., pneumonic type); and intrapulmonary metastasis (9). With the popularization of CT screening, patients with multiple nodules of less
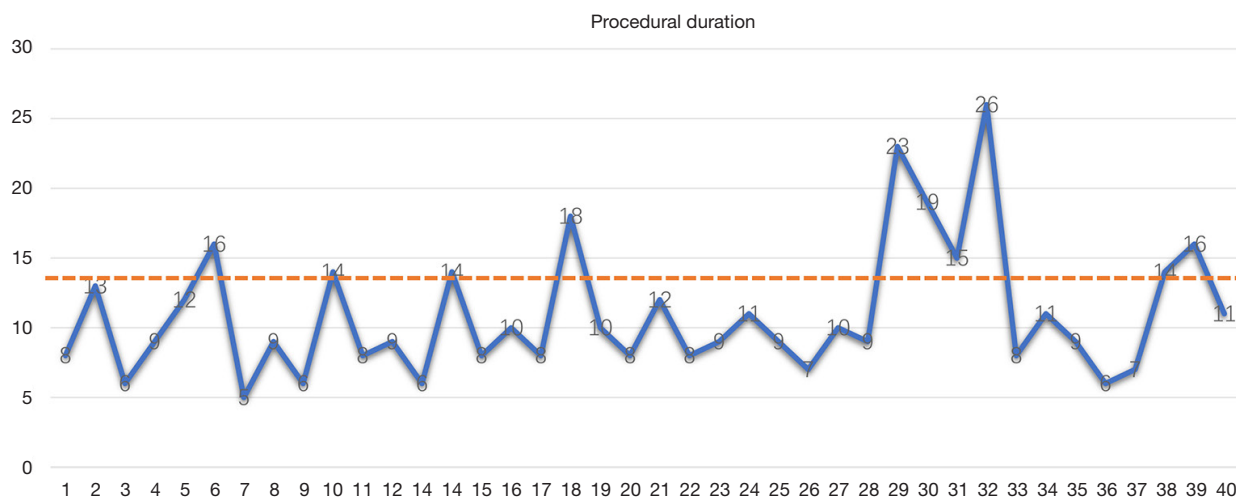
　　　Transl Lung Cancer Res 2021;10(3):1474-1483 | http://dx.doi.org/10.21037/tlcr-21-202

Table 1 Patient characteristics

Variables	Values
Sex, n (%)	40
Female	31 (77.5)
Male	9 (22.5)
Age (year), mean ± SD	53.5±8.5
Diameter (mm), mean ± SD[†]	9.8±4.2
Distance from pleura, mm (IQR)	8.2 (4.8, 11)
No. of lesions on CT, n (%)	126
pGGN	98 (77.8)
PSN	18 (14.3)
Pure solid nodule	10 (7.9)
Nodule location, n (%)	126
RUL	52 (41.3)
RML	12 (9.5)
RLL	24 (19)
LUL	11 (8.7)
LLL	27 (21.4)

[†], diameter, the largest dimension of the invasive component was measured for T category according to the 8th edition TNM staging. SD, standard deviation; IQR, interquartile range; mm, millimeter; pGGN, pure ground-glass nodule; PSN, partial solid nodule; AAH, atypical adenomatous hyperplasia; AIS, adenocarcinoma in situ; MIS, microinvasive adenocarcinoma; RUL, right upper lobe; RML, right middle lobe; RLL, right lower lobe; LUL, left upper lobe; LLL, left lower lobe.

than 1 cm are being diagnosed with increasing frequency. Sometimes, the lesions of a patient may contain both intrapulmonary metastasis and heterogeneous multiple primary lung cancer nodules. Thus, reliable methods to locate all nodules in resected specimens are urgently needed by surgeons and pathologists.

To date, various localization methods have been reported, including preoperative and intraoperative radio-guided detection, intraoperative ultrasound, and electromagnetic navigation (10-12). Preoperative CT-guided percutaneous fine-needle localization is an invasive operation, which may cause hemorrhage, pneumothorax, tumor translocation, and other complications (13). Moreover, not all cases are suitable for this method due to the position of lesions. Intraoperative ultrasound and electromagnetic navigation require the operator to be experienced and proficient in endoscopic devices. Besides, some special medical equipment is needed. Li *et al.* reported that CT-guided location of lesions in surgical specimens using fine needles under constant, moderate mechanical aeration allows for the rapid and accurate localization of lesions (14). However, this method has considerable limitations and its popularization in clinical practice is challenging. The success of their approach is highly dependent on the airway integrity of the surgical specimens. Thus, it requires inflatable aerator and CT scanner. The fact that the precise locations of multiple nodules are not usually indicated clearly in the pathological report greatly hinders retrospective studies of multiple primary lung cancer that are yet to be carried out, and this

Figure 5 Procedural duration of each cases. The red dotted line indicates the mean time.

Transl Lung Cancer Res 2021;10(3):1474-1483 | http://dx.doi.org/10.21037/tlcr-21-202

is deserving of more attention. Therefore, reference to the imaging information of each nodule is of great significance to improving the accuracy of pathological sampling and diagnosis.

If the nodules are not peripheral pulmonary lesions, then determining the pathological location of most GGNs in resected specimens is difficult. Moreover, it is harder to accurately identify the positions of these GGNs when they are located in the same lobe or segment, especially if they

are adjacent to each other. At worst, the thoracic surgeon may be unable to find the nodule in the resected specimen, and serial sectioning of the whole specimen may be required to check for possible lesions. This scenario is a drain on time, and might even affect the scope of a given operation, pathological diagnosis, or the subsequent treatment strategy of the patient (15). With the auxiliary of 3D reconstruction/printing, we successfully located lesions in the resected specimens of all 40 cases. The important guiding significance of this method in the pathological location of multiple pulmonary nodules in resected specimens can be summarized as follows: (I) 3D reconstruction/printing models can improve the positive rate of pathological sampling of multiple pulmonary nodules; (II) through 3D reconstruction, the description of the position of nodules is more accurate and comprehensive than that in pathological reports; (III) 3D reconstruction/printing models can be used as a well-tried intermediate tool to match CT imaging features with the pathological features of multiple pulmonary nodules; (IV) 3D reconstruction/printing models can aid pathologists in gaining an understanding the characteristics of lesions in their entirety. The possible reasons why 2 of the pGGNs in this study could not be located is that the nodules were too small to be found in their respective specimens. However, given they were secondary lesions and lobectomy was performed for main foci, the failure to locate them did not affect the patients' subsequent diagnosis and treatment.

It cannot be denied that there are still some limitations to this study. First of all, 3D reconstruction/printing is not suitable for wedge resection specimens, as they lack anatomical landmarks. Secondly, considering the expense of 3D printing model, further study should be implemented to evaluate the cost-effectiveness of 3D printing model.

Table 2 Pathological and surgical outcomes

Variables	Values
Pathological finding	
No. of detected lesions, n (%)	124
AAH	11 (8.9)
AIS	47 (37.9)
MIS	25 (20.2)
Squamous cell carcinoma	4 (3.2)
Adenocarcinoma	32 (25.8)
Benign	5 (4.0)
Lymph node, n (%)	
Positive	1 (2.5)
Negative	39 (97.5)
Procedural duration (min), mean ± SD	11±4.6
Type of surgery, n (%)	
Segmentectomy	27 (67.5)
Lobectomy or with segmentectomy	13 (32.5)

AAH, atypical adenomatous hyperplasia; AIS, adenocarcinoma in situ; MIA, microinvasive adenocarcinoma; SD, standard deviation.
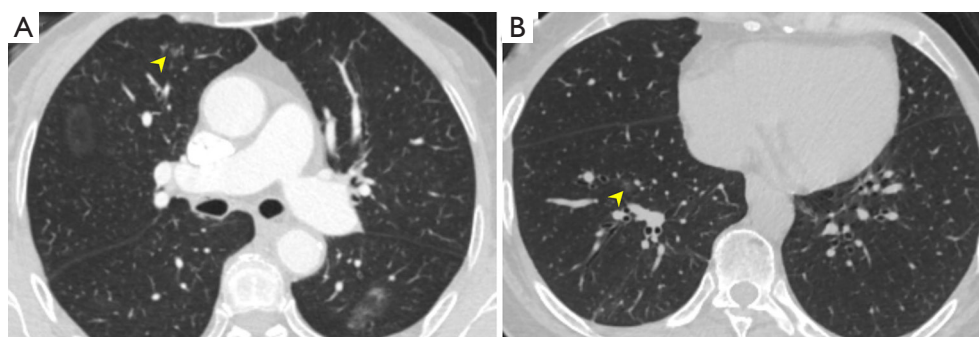

Figure 6 Two nodules were not found in surgical specimens (shown via yellow arrows). (A) A pure ground glass nodule in the right upper lobe; (B) a pure ground glass nodule in the right lower lobe.

Conclusions

In conclusion, we showed that locating multiple nodules in resected specimens with the auxiliary of 3D reconstruction has the success rate of 98%. This method represents novel progress in pathological sampling of multifocal pulmonary nodules and may have widespread availability. Furthermore, the excellent agreement between the pathological results of the samples and their CT images will provide assistance for future studies on the pathological characteristics and radiomics of multiple primary lung tumors.

Footnote

Reporting Checklist: The authors have completed the STROBE reporting checklist. Available at http://dx.doi.org/10.21037/tlcr-21-202

Data Sharing Statement: Available at http://dx.doi.org/10.21037/tlcr-21-202

Conflicts of Interest: All authors have completed the ICMJE uniform disclosure form (available at http://dx.doi.org/10.21037/tlcr-21-202). The authors report that receive only technological supports from Zhen Yuan (Tianjin) Medical Device Technology Co., Ltd., with no known financial stake. The other authors have no conflicts of interest to declare.

Ethical Statement: The authors are accountable for all aspects of the work in ensuring that questions related to the accuracy or integrity of any part of the work are appropriately investigated and resolved. This study was approved by the ethics committee of the National Cancer Center/Cancer Hospital, Chinese Academy of Medical Sciences and Peking Union Medical College (approval no. 20/130-2326). Informed consent was taken from all the patients.

Open Access Statement: This is an Open Access article distributed in accordance with the Creative Commons Attribution-NonCommercial-NoDerivs 4.0 International License (CC BY-NC-ND 4.0), which permits the non-commercial replication and distribution of the article with the strict proviso that no changes or edits are made and the original work is properly cited (including links to both the formal publication through the relevant DOI and the license). See: https://creativecommons.org/licenses/by-nc-nd/4.0/.

References

1. Smith RA, Andrews KS, Brooks D, et al. Cancer screening in the United States, 2019: A review of current American Cancer Society guidelines and current issues in cancer screening. CA Cancer J Clin 2019;69:184-210.
2. Wender RC, Brawley OW, Fedewa SA, et al. A blueprint for cancer screening and early detection: Advancing screening's contribution to cancer control. CA Cancer J Clin 2019;69:50-79.
3. Asamura H. Multiple primary cancers or multiple metastases, that is the question. J Thorac Oncol 2010;5:930-1.
4. Tanvetyanon T, Boyle TA. Clinical implications of genetic heterogeneity in multifocal pulmonary adenocarcinomas. J Thorac Dis 2016;8:E1734-8.
5. Vazquez M, Carter D, Brambilla E, et al. Solitary and multiple resected adenocarcinomas after CT screening for lung cancer: histopathologic features and their prognostic implications. Lung Cancer 2009;64:148-54.
6. Zhang Z, Gao S, Mao Y, et al. Surgical Outcomes of Synchronous Multiple Primary Non-Small Cell Lung Cancers. Sci Rep 2016;6:23252.
7. Travis WD, Brambilla E, Noguchi M, et al. International association for the study of lung cancer/American thoracic society/European respiratory society international multidisciplinary classification of lung adenocarcinoma. J Thorac Oncol 2011;6:244-85.
8. Shimizu S, Yatabe Y, Koshikawa T, et al. High frequency of clonally related tumors in cases of multiple synchronous lung cancers as revealed by molecular diagnosis. Clin

Cancer Res 2000;6:3994-9.

9. Li H. Overview of The AJCC Lung Cancer Staging System, Eighth Edition may give us more thought: opportunities and challenges. Zhonghua Wai Ke Za Zhi 2017;55:346-50.

10. Nakano N, Miyauchi K, Imagawa H, et al. Immediate localization using ultrasound-guided hookwire marking of peripheral lung tumors in the operating room. Interact Cardiovasc Thorac Surg 2004;3:104-6.

11. Kleedehn M, Kim DH, Lee FT, et al. Preoperative Pulmonary Nodule Localization: A Comparison of Methylene Blue and Hookwire Techniques. AJR Am J Roentgenol 2016;207:1334-9.

12. Long J, Petrov R, Haithcock B, et al. Electromagnetic Transthoracic Nodule Localization for Minimally Invasive Pulmonary Resection. Ann Thorac Surg 2019;108:1528-34.

13. Wu CC, Maher MM, Shepard J-AO. Complications of CT-guided percutaneous needle biopsy of the chest: prevention and management. AJR Am J Roentgenol 2011;196:W678-82.

14. Li M, Shen G, Gao F, et al. CT-guided fine-needle localization of ground-glass nodules in re-aerated lung specimens: localization of solitary small nodules or multiple nodules within the same lobe. Diagn Interv Radiol 2015;21:391-6.

15. Chen W, Chen L, Qiang G, et al. Using an image-guided navigation system for localization of small pulmonary nodules before thoracoscopic surgery: a feasibility study. Surg Endosc 2007;21:1883-6.

Title

Application of 3D reconstruction/3D printing model in pathological sampling of multifocal pulmonary nodules: a prospective single-arm study

Grant

National Key R&D Program of China (2017YFC1308700)

Principal Investigator

Shugeng Gao

Sponsor

National Cancer Center/National Clinical Research Center for Cancer/Cancer Hospital, Chinese Academy of Medical Sciences and Peking Union Medical College

Version Number: 1.0
2019/08/21

Statement of compliance

The study will be conducted in accordance with Declaration of Helsinki, International Conference on Harmonization guidelines for Good Clinical Practice (ICH E6) and Medical Equipment Specification for the Quality Control of Clinical Trial (State Food and Drug Administration/National Health and Family Planning Commission/Number twenty-fifth). All personnel involved in the conduct of this study have completed human subject protection training.

Signature page

The signature below constitutes the approval of this protocol and provides the necessary assurances that this trial will be conducted according to all stipulations of the protocol, including all statements regarding confidentiality, and according to local legal and regulatory requirements.

Principal Investigator:
Signed: Date:
Name: Shugeng Gao
Title: MD.

Protocol summary

Title: Application of 3D reconstruction/3D printing model in pathological sampling of multifocal pulmonary nodules: a prospective single-arm study.

Objective: To evaluate the effectiveness of 3D reconstruction/3D printing technology in the pathological collection of surgical specimens of multiple lung nodules.

Participants: Patients aged 18–79 years old; with thin-slice CT showed multiple pulmonary nodules, planning to perform lung lobe/pulmonary segment surgery; two or more nodules are present in the same lobe or segment; the largest diameter of the lung window of the main lesion is 0< d ≤20 mm; with clinical staged I (cT1N0) (UICC-TNM edition 8); ECOG scored 0–1; without history of the following operations: ipsilateral thoracotomy, ipsilateral thoracoscopic lung and esophagectomy, mediastinal surgery (except for bullae and rib fractures), contralateral thoracotomy or thoracoscopic surgery (except for bullae and rib fractures); without preoperative neoadjuvant treatment; no history of radiotherapy; all patients have complete preoperative examinations: chest and upper abdomen CT, neck ultrasound (neck, supraclavicular lymph nodes) and abdominal ultrasound (liver, gallbladder, pancreas, spleen, Both kidneys, adrenal glands) examination, cranial MRI, bone scan (PET-CT can replace ultrasound, cranial MRI and bone scan). Sign informed consent.

Number of site: This is a single-center trial and all participants would be recruited in National Cancer Center/National Clinical Research Center for Cancer/Cancer Hospital, Chinese Academy of Medical Sciences and Peking Union Medical College.

Description of Intervention: The study will not affect the patient's surgical treatment process.

Estimated Study Duration: From 2019. 09 to 2020.09.

Estimated Time to Complete Enrollment: 2020.06

Schematic of Study Design

3D: three-dimensional
CT: computed tomography
GGO: ground glass nodule
VATS: video assisted thoracoscopic surgery

Introduction: background information and scientific rationale

Background information

Since the middle of the 20th century, more and more evidence support tumor screening, which has made a significant contribution to the detection and treatment of early disease (1,2). With the improvement of people's awareness of cancer prevention and the clinical application of high-resolution CT (HRCT), patients with early multiple pulmonary nodules have gradually increased (3-5). The CT findings of these patients are mostly pure ground glass nodules (pGGNs) or mixed density ground glass nodules (mGGNs). Surgical treatment can not only preserve lung function to the greatest extent, but also enable most patients to receive effective radical treatment. For early multifocal pulmonary nodules, wedge resection, lobectomy or selective segmental resection should be selected according to the specific situation. In addition, surgical specimens can provide more detailed pathological and genetic characteristics for adjuvant treatment and follow-up monitoring of multiple primary lung cancers (6,7).

A key issue of simultaneous multiple primary lung cancer is the choice of surgical methods. Due to the lack of prospective clinical trials and consistent diagnostic criteria, there is no unified consensus on the treatment criteria for multiple primary lung cancers (MPLCs). At present, there is no clear guideline for the diagnosis and treatment of simultaneous multiple primary lung cancer (sMPLC). The scope of surgical resection is mainly based on the patient's surgical risk and the surgeon's personal choice. Although some cases have been reported in the SEER database, the National Cancer Database (NCDB) of the United States, and European and Asian databases, and some treatment strategies and recommendations have been proposed, due to the controversy caused by individual differences between patients, the three major lung cancer research institutions [International Union Against Cancer (UICC), American Joint Committee on Cancer (AJCC) and International Association for the Research of Lung Cancer (IALSC)] did not agree on this consensus. The choice of surgical strategy for simultaneous multiple primary lung cancers mainly depends on the diagnosis of CT before operation.

In recent years, with the development and application of 3D reconstruction technology, treatment strategies for early lung cancer are gradually changing. For patients with early-stage lung cancer less than 2 cm, segmentectomy has become a feasible radical operation. For patients with multiple primary lung cancers, due to the influence of the number and location of the lesions, it may be difficult to plan the surgical strategy solely relying on CT judgment. Therefore, it is necessary to further evaluate the impact of three-dimensional reconstruction technology on the surgical strategy of multiple pulmonary nodules, and provide feasible suggestions and help for the surgical treatment of sMPLC. For multiple pulmonary nodules surgical specimens, the reliability of tissue specimen sampling depends on the precise positioning of each nodule. If the pathologist can accurately describe the types and characteristics of different nodules under the microscope, it will help clarify the nature of multiple lesions and this has guiding significance for tumor staging (multiple primary or lung metastasis). In addition, if the pathology report can be matched with the preoperative CT image one by one, it will help to carry out the research on the imaging and pathological characteristics of multiple primary lung cancers in the future, and benefit for the selection of appropriate treatment methods (observation, wedge resection, selection Segmental resection or lobectomy, etc.). However, in the actual operation process, due to the lack of sufficient understanding of preoperative CT images, unless the thoracic surgeon identifies all the lesions, it is difficult for the pathologist to find lesions during the process of collecting materials. At the same time, due to the lack of accurate pathological material location, the pathology report of early multiple nodules rarely corresponds to the preoperative image one-by-one, and it is difficult to retrospectively evaluate the characteristics of each nodule. Therefore, we need a method that can not only help the surgeon locate the nodules, but also help the pathologist locate all the nodules and diagnose each nodule (7).

The 3D reconstruction/3D printing model provides us with a good cross-reference method to guide surgeons and pathologists to locate multiple lesions in the specimen. This study aims to explore the application value of 3D reconstruction and 3D printing models in the surgical treatment of simultaneous multiple pulmonary nodules. It hopes to provide feasible suggestions on the selection of early multiple primary lung cancer surgery strategies and

pathological materials, and provide evidence support for the superiority of three-dimensional reconstruction technology in the early multiple primary lung cancer surgical treatment.

Potential risk and benefits

Potential risks

The study does not affect the surgical treatment process of patients. 3D reconstruction will not affect the patient's treatment process. Therefore, complications are only related to the operation itself. 3D reconstruction does not increase potential risk of patients.

Potential Benefits

Based on our previous experience, the application of 3D reconstruction technology in multiple nodule localization in resected specimens might facilitate the process of nodule localization. For multiple nodules on the same lobe or segment, it is difficult to find all the lesions for surgeons or pathologists. In addition, due to the lack of accurate pathological material location, the pathology report of early multiple nodules rarely corresponds to the preoperative image one-by-one, thus it is difficult to retrospectively evaluate the characteristics of each nodule. Instead, the 3D reconstruction/3D printing model provides us with a good cross-reference method to guide surgeons and pathologists to locate multiple lesions in the specimen. In this way, surgeons and pathologists can locate nodules accurately on the resected specimens, which convenient for the correspondence of the nodule pathology and CT image features. At the same time, surgical procedures are performed safer under the assistant of 3D reconstruction/3D printing model.

Objectives

Study objectives

To evaluate the effectiveness of 3D reconstruction/3D printing technology in the pathological collection of surgical specimens of multiple lung nodules.

Study outcomes

Primary outcome: the success rate and accuracy rate of surgical specimen collection using 3D printing model.

Secondary outcome: the agreement rate between the pathological results of the samples and CT images after using 3D printing model to collect material.

Study design

The basic idea

Use the univariate single-group design to clarify the success rate and accuracy of the 3D reconstruction technology assisted pathology specimen sampling.

Study population and groups

Patients enrolled in this study were performed 3D reconstruction according to preoperative CT. In this single-arm clinical trial, anatomic lobectomy or segmentectomy will be performed for all patients. To assure that the assigned surgical procedures are performed properly, the procedures will be centrally reviewed by principal investigator (SG Gao) and the lead implementer (B Qiu). The process of localizing nodules in surgical specimens will be performed by researchers of the project team. This process will be aided by 3D reconstruction image or 3D printing model.

3D printing model preparation and surgical process

(I) 3D printing model preparation: Obtain the preoperative CT data of the first enrolled patients from the workstation of the imaging department of our hospital. Import the DICOM data of thin-slice (0.625–1.25 mm) CT images into Mimics software (Materialise's interactive medical image control system) to perform three-dimensional reconstruction. Planning the resection area and cutting plane in the three-dimensional image, this process is completed by the thoracic surgeon in the research team. Subsequently, 3-Matic software is used to process the "stereolithography (STL)" format of the reconstructed image, and then print the 3D model. This process is assisted by a third-party company [Zhen Yuan (Tianjin) Medical Device Technology Co., Ltd].

(II) Surgical process: The study does not affect the surgical treatment process of patients. The patient received video-assisted thoracoscopic lobectomy or anatomical partial lobectomy, double-lumen endotracheal intubation ventilation, general anesthesia, and contralateral ventilation single-port/three-port thoracoscopic surgery. The three-hole method makes a 1.0 cm incision at the mid-axillary line of the patient's 7th and 8th intercostal

space. The observation hole is reasonably inserted into the thoracoscope. Choose the 3.0 cm incision at the anterior axillary line between the 3th or 4th intercostals as the main operation hole, and the 2.0 cm incision at the lower line of the shoulder armor between the 7th or 8th intercostals as the auxiliary handle control operation. The single-hole method uses a 3–5 cm incision at the patient's 4th or 5th intercostal anterior axillary line as an observation/operation hole. Perform standard lobectomy or anatomical partial lobectomy on the patient. Fine thread ligation is performed for the smaller blood vessel branches, and the staple cartridge of the linear cutting stapler is selected for the thick lung tube to completely stop the bleeding and complete the operation. Observe and monitor the vital signs of patients strictly during and after surgery.

The process of localizing nodules in surgical specimens

This process is completed by surgeons and pathologists. The resected surgical specimens are compared with the preoperative 3D reconstruction/3D printing model, and the lesions are found and marked in the resected surgical specimens according to the position of the nodules identified on the 3D reconstruction. The thoracic surgeon assists the pathologist to locate the nodules, and once a lesion is found, it is marked with the corresponding Roman numeral (#1, #2, #3...) in the 3D printed model, and the pathologist performs the corresponding operation specimen mark registration. Subsequently, the pathological diagnosis process was carried out in accordance with the routine pathology procedure. After the pathology report is reported, according to the number sequence of the nodules in the pathology report, using the 3D printing model as an intermediary, the pathological diagnosis of the nodules and the location of the lesion in the CT image are one-to-one correspondence. If the nodule marked in the 3D printing model is not found in the surgical specimen, mark 'NO' on the model. Finally, calculate the success rate of all enrolled patients (the actual number of nodules * 100%/3D printing model number of nodules), and the corresponding rate of nodules and preoperative CT (the lesions in the postoperative pathology report can be Corresponding to the number of nodules on the preoperative CT*100%/total number of lesions in the postoperative pathology report).

Time schedule

The trail is planned to start in October 2019 and complete before September 2020.

Statistical analysis

Sample size estimation: α (inspection level) is set to 0.05, 1-β (inspection power) is set to 0.8, the experimental group rate value is set to 0.95, the reference rate value is based on the previous multiple nodules surgery specimens in our department The accuracy rate and the corresponding rate of the preoperative CT image were set to 0.7, and the Δ (cutoff value) was set to 0.1. The algorithm uses Z-pooled approximate estimation method to perform high-quality estimation, and the calculated sample size is n=32. Because there may be unqualified cases due to various reasons, the sample size increases by 10–20%, and the final sample size N=40 cases.

Study enrollment and withdraw

Inclusion criteria for the first (pre-operative) registration

For inclusion in the first (pre-operative) registration, patients will be required to fulfill all of the following criteria: (I) patients aged 18–79 years old; (II) with thin-slice CT showed multiple pulmonary nodules, planning to perform lung lobe/pulmonary segment surgery; (III) the largest diameter of the lung window of the main lesion is 0< d ≤20 mm; (IV) two or more nodules are present in the same lobe or segment; (V) with clinical staged I (cT1N0) (UICC-TNM edition 8); (VI) ECOG scored 0–1; (VII) without history of the following operations: ipsilateral thoracotomy, ipsilateral thoracoscopic lung and esophagectomy, mediastinal surgery (except for bullae and rib fractures), contralateral thoracotomy or thoracoscopic surgery (except for bullae and rib fractures); (VIII) without preoperative neoadjuvant treatment; (IX) no history of radiotherapy; (X) all patients have complete preoperative examinations: chest and upper abdomen CT, neck ultrasound (neck, supraclavicular lymph nodes) and abdominal ultrasound (liver, gallbladder, pancreas, spleen, Both kidneys, adrenal glands) examination, cranial MRI, bone scan (PET-CT can replace ultrasound, cranial MRI and bone scan); (XI) sign informed consent.

Exclusion criteria

(I) Taking other experimental drugs at the same time or in other clinical trials; (II) preoperative examination results

are considered as metastatic lesions; (III) pregnant/lactating female patients; (IV) people without legal capacity, medical or ethical the cause affects those who continue the study.

Inclusion criteria for the secondary (intra-operative) registration

(I) The patient underwent lobectomy or segmentectomy; (II) the patient prepared 3D reconstruction/printing model.

Exclusion criteria for the secondary (intra-operative) registration

(I) Conversion to wedge resection during the operation.

Shedding standard

(I) The patient does not follow-up the study according to the procedure after he/she signed the informed consent; (II) after the patient was enrolled, the operation was performed in other hospital.

Rejection criteria

(I) The data of the enrolled patients are missing or incorrect due to human/objective reasons; (II) after registration, the research group found that the patient concealed illness.

Study intervention

This trial is mainly designed to confirm that 3D reconstruction can be benefit to pathological sampling in resected specimens which contains multiple lesions. Therefore, all nodule localization procedures in resected specimens are performed under the auxiliary of 3D reconstruction images and 3D printing models [Zhen Yuan (Tianjin) Medical Device Technology Co., Ltd]. After successful nodule localization, the nodule will be signed by silk thread. Then the signed nodule is marked with the corresponding Roman numeral (#1, #2, #3…) in the 3D printed model.

Ethics and protection of human subjects

Ethical standard

The investigator will ensure that this study is conducted in full conformity with the rules set by the Medical Equipment

Specification for the Quality Control of Clinical Trial (*State Food and Drug Administration/National Health and Family Planning Commission/Number twenty-fifth*). All personnel involved in the conduct of this study have completed human subject protection training.

Institutional review board

The protocol, informed consent form(s), recruitment materials, and all subject materials will be submitted to the IRB (*National Cancer Center/National Clinical Research Center for Cancer/Cancer Hospital*, *Chinese Academy of Medical Sciences and Peking Union Medical College*) for review and approval. Approval of both the protocol and the consent form must be obtained before any subject is enrolled. Any amendment to the protocol will require review and approval by the IRB before the changes are implemented in the study.

Informed consent process

Before the participants agree to participate into the trial, Informed consent is obtained in the study and continues throughout study participation. A consent form describing in detail the study procedures and related risks would be given to the subject before participation. Consent forms will be IRB-approved, and the subject is required to read and review the document or have the document read to him or her. The investigator or designee will explain the research study in detail to the participants and answer any questions that may arise. Subjects will sign the informed consent document before any study-related assessments or procedures. Subjects will be given the opportunity to discuss the study with their surrogates or think about it prior to agreeing to participate. They may withdraw consent at any time throughout the course of the study. A copy of the signed informed consent document will be given to subjects for their records. The rights and welfare of the subjects will be protected by emphasizing to them that the quality of their clinical care will not be adversely compromised if they refuse to participate in this trial. The consent process will be documented in the clinical or research record.

Data storage policy

The principal investigator is responsible for ensuring the accuracy, completeness, legibility, and timeliness of the data reported. All source documents should be completed in a neat, legible manner to ensure accurate interpretation

of data. The investigators need to maintain adequate case histories of study subjects, including accurate case report forms (CRFs) and source documentation.

Data collection and accurate documentation are the responsibilities of the study staff under the supervision of the primary investigator. All source documents, laboratory results and CT images must be reviewed by the study team and data entry staff, who will ensure that they are accurate and complete. Unanticipated problems and adverse events must be reviewed by the primary investigator.

All the study documents and records should be stored for a minimum of 2 years after trial completion, which is required by the Medical Equipment Specification for the Quality Control of Clinical Trial (State Food and Drug Administration/National Health and Family Planning Commission/Number twenty-fifth). No trial documents should be deliberately destroyed or damaged without consent of the IRB.

Table S1 Patients' detailed information

Patient no.	Age (years)/sex	No. of lesions	Size (mm)	CT finding	Treatment	Pathologic finding	Lymph node	Distance from the visceral pleura to the nodule* (mm)
1	58/M	1	14	pGGO	RS1a + S2b + S3ai	MIS	0	9
		2	18	PSN		Adenocarcinoma		11
		3	3	pGGO		AIS		4
2	62/F	1	13	pGGO	RS3b	MIS	0	3
		2	4	pGGO		AIS		6
3	51/F	1	8	pGGO	LS6 + S9a + S10a	Adenocarcinoma	0	5
		2	4	pGGO		AIS		6
4	43/F	1	18	PSN	RUL	Adenocarcinoma	0	12
		2	7	pGGO		AIS		9
5	52/F	1	5	pGGO	RS3	MIS	0	4
		2	5	pGGO		MIS		7
6	43/F	1	5	pGGO	RS4 + RS1 + S6	AIS	0	6
		2	6	pGGO		AIS		9
		3	8	pGGO		MIS		2
7	55/M	1	15	PSN	LLL	Adenocarcinoma	0	7
		2	8	pGGO		Adenocarcinoma		11
8	50/F	1	4	pGGO	S2b + S3aii	AAH	0	4
		2	5	pGGO		AAH		6
9	65/M	1	17	PSN	LS6	Adenocarcinoma	0	7
		2	4	PSN		granuloma		12
10	50/M	1	5	pGGO	RS1	AAH	0	8
		2	20	Pure solid nodule		Reactive lymph node hyperplasia		1
11	54/F	1	10	pGGO	LS10	Adenocarcinoma	0	3
		2	5	pGGO		MIS		11
12	45/F	1	10	PSN	RS1 + S2	Adenocarcinoma	0	14
		2	4	pGGO		AIS		7
		3	8	pGGO		AIS		8
13	57/F	1	9	Pure Solid Nodule	LLL	Adenocarcinoma	0	4
		2	4	pGGO		Adenocarcinoma		8
14	47/M	1	9	PSN	RUL + S6	Adenocarcinoma	0	9
		2	4	pGGO		MIS		13
		3	3	pGGO		AIS		11
		4	4	pGGO		AIS		3
15	70/M	1	11	PSN	RS8	Adenocarcinoma	0	15
		2	3	Pure solid nodule		AAH		2
16	67/M	1	13	PSN	LS3 + S4 + S5	Adenocarcinoma	0	17
		2	4	pGGO		AAH		11
		3	3	pGGO		AAH		9
17	33/F	1	7	pGGO	RS9b + S3a	MIS	0	14
		2	4	pGGO		AAH		11
		3	4	pGGO		AAH		4
18	47/F	1	6	pGGO	LS6b + 8a	MIS	0	3
		2	2	pGGO		AIS		8
		3	4	pGGO		AIS		2
		4	3	pGGO		AIS		5
		5	6	pGGO		AIS		7
		6	4	pGGO		AIS		5
19	48/F	1	8	pGGO	LS1 + 2	MIS	0	22
		2	11	pGGO		MIS		10
20	54/F	1	9	PSN	RML	Adenocarcinoma	0	4
		2	3	pGGO		MIS		2
		3	2	pGGO		AAH		3
		4	2	Pure solid nodule		AAH		1
21	61/F	1	18	PSN	LS1 + 2c + S3a	Adenocarcinoma	0	12
		2	10	pGGO		Adenocarcinoma		8
		3	3	pGGO		AIS		6
		4	3	pGGO		AIS		9
22	42/F	1	5	pGGO	LS10	AIS	0	13
		2	6	pGGO		AIS		2
23	57/F	1	7	pGGO	RS3 + S5 + S6	Adenocarcinoma	0	1
		2	5	pGGO		AIS		23
		3	3	pGGO		AIS		5
		4	2	Pure solid nodule		AIS		4
		5	8	pGGO		MIS		3
24	44/F	1	18	PSN	RUL	squamous cell carcinoma	0	23
		2	4	pGGO		squamous cell carcinoma		3
		3	3	pGGO		squamous cell carcinoma		5
		4	5	pGGO		squamous cell carcinoma		5
25	55/F	1	5	pGGO	LS8a + 9a	AIS	0	4
		2	6	pGGO		AIS		8
26	49/F	1	17	PSN	RUL	Adenocarcinoma	0	23
		2	10	pGGO		Adenocarcinoma		12
27	46/M	1	5	pGGO	RS3	MIS	0	10
		2	4	pGGO		MIS		2
28	60/F	1	7	PSN	LS6	Adenocarcinoma	0	7
		2	4	pGGO		AIS		5
29	58/F	1	8	pGGO	RLL	Adenocarcinoma	N1	2
		2	12	pGGO		Adenocarcinoma		5
		3	6	pGGO		Adenocarcinoma		3
		4	20	Pure solid nodule		Adenocarcinoma		18
		5	3	Pure solid nodule		Benign		0
		6	5.8	pGGO		Not found		
30	66/M	1	5	pGGO	RUL	AIS	0	8
		2	4	pGGO		AIS		14
		3	16	Pure solid nodule		Benign		17
		4	8	pGGO		AIS		9
		5	14	pGGO		Adenocarcinoma		3
		6	6	pGGO		MIS		8
		7	5	pGGO		MIS		6
31	44/F	1	10	pGGO	RS6b + S1 + S3b	MIS	0	8
		2	2	pGGO		AIS		8
		3	4	pGGO		AIS		10
		4	4	pGGO		AIS		16
		5	5	pGGO		AIS		7
		6	5	pGGO		AIS		3
		7	3	pGGO		AIS		8
32	67/F	1	10	pGGO	RUL	Adenocarcinoma	0	32
		2	4	Pure solid nodule		MIS		2
		3	12	pGGO		MIS		8
		4	14	PSN		Adenocarcinoma		5
		5	9	pGGO		Adenocarcinoma		9
		6	4.2	pGGO		Not found		
33	56/M	1	8	pGGO	RS3 + 1b	AIS	0	7
		2	3	pGGO		AIS		10
34	61/F	1	15	pGGO	RML + S6	MIS	0	8
		2	17	PSN		Adenocarcinoma		12
		3	5	pGGO		AIS		6
35	64/F	1	18	PSN	RUL	Adenocarcinoma	0	24
		2	7	pGGO		AIS		13
		3	4	pGGO		AAH		3
36	56/F	1	8	pGGO	RS6b + S8a + S9a	AIS	0	5
		2	4	pGGO		AIS		8
37	50/F	1	8	pGGO	LS4 + S5	Adenocarcinoma	0	6
		2	10	Pure solid nodule		granuloma		14
38	50/F	1	8	PSN	RML	Adenocarcinoma	0	22
		2	2	pGGO		MIS		6
		3	3	pGGO		MIS		8
		4	4	pGGO		AIS		5
39	59/F	1	4	pGGO	LS6c + S9 + S10	AIS	0	9
		2	5	pGGO		AIS		9
		3	5	pGGO		AIS		6
		4	6	pGGO		AIS		8
		5	13	pGGO		AIS		9
40	42/F	1	5	pGGO	RS1 + S2 + S6	AIS	0	13
		2	5	pGGO		MIS		15
		3	6	pGGO		MIS		8

*, distance from the visceral pleura to the nodule: measured on specimens. pGGO, pure ground-glass opacity; PSN, partial solid nodule; RUL, right upper lobectomy; RML, right middle lobectomy; RLL, right lower lobectomy; LLL, left lower lobectomy; AAH, atypical adenomatous hyperplasia; AIS, adenocarcinoma in situ; MIS, microinvasive adenocarcinoma.